INSTITUTE OF PHYSICS PUBLISHING JOURNAL OF PHYSICS B: ATOMIC, MOLECULAR AND OPTICAL PHYSICS

J. Phys. B: At. Mol. Opt. Phys. **39** (2006) S1229–S1239 doi:10.1088/0953-4075/39/19/S29

Quenching of rotationally excited CO in cold and ultracold collisions with H, He and H_2

Benhui Yang[1], **Hemamali Perera**[2], **N Balakrishnan**[2], **R C Forrey**[3] **and P C Stancil**[1]

[1] Department of Physics and Astronomy and The Center for Simulational Physics, The University of Georgia, Athens, GA 30602, USA
[2] Department of Chemistry, University of Nevada Las Vegas, Las Vegas, NV 89154, USA
[3] Department of Physics, Penn State University, Berks-Lehigh Valley College, Reading, PA 19610, USA

E-mail: yang@physast.uga.edu

Received 31 March 2006
Published 25 September 2006
Online at stacks.iop.org/JPhysB/39/S1229

Abstract
The study of molecular inelastic collision processes at cold and ultracold temperatures is of considerable interest as schemes are currently being developed to efficiently cool and trap neutral polar molecules. In this work, quantum-mechanical scattering calculations are presented for the quenching of rotationally excited CO due to collisions with H, He and H_2 for collision energies between 10^{-5} and $10\,\mathrm{cm}^{-1}$. The calculations were performed using the close-coupling approach and the coupled-states approximation. Cross sections for the quenching of the $j = 1$–10, 20, 30 and 40 levels of CO are presented and mechanism and trends of energy transfer in these systems are discussed.

1. Introduction

Experimental advances in cooling and trapping of cold atoms have stimulated research aiming at the creation of cold molecules [1, 2]. The availability of cold and ultracold molecules may open routes to many new applications such as condensation of complex molecular systems, coherent control of molecular collisions towards ultracold chemistry, and precision measurements of molecular interactions. In the past decade, several methods have been developed to cool and trap molecules at cold and ultracold temperatures. The helium buffer gas cooling technique [3] has proven to be effective in loading molecules into a magnetic trap [4] and it has been shown that the method may be used to create a cold molecular beam [5]. Such a molecular beam in conjunction with an atomic condensate could be used to investigate atom–molecule collisions at cold and ultracold temperatures. Another approach for the production of ultracold molecules involves photoassociation of laser-cooled atoms [6–8] which generally yields molecules with translational temperatures in the μK

regime. However, molecules created by this technique are in highly excited vibrational levels and collisional quenching of these molecules limits their lifetimes. A similar approach using a magnetic field (magnetoassociation) has been successful in creating molecular Bose–Einstein condensates (BECs) of fermionic atoms using the Feshbach resonance technique [9–12]. In this approach, the magnetic field is scanned across a Feshbach resonance during which a pair of interacting atoms are converted to molecules. The resulting molecules are also highly vibrationally excited as in the photoassociation technique but they are more stable against collisional decay due to Pauli blocking. For polar molecules, the Stark decelerator method [13, 14] has proven to be very useful. The method uses a time-varying electric field to slow molecules and it is applicable to a broad range of molecular systems with permanent dipole moments. Applications of this technique to cool and trap metastable CO [13], deuterated ammonia [15] as well as the OH radical [16] have been demonstrated.

The possibility of cooling and trapping molecules provides a unique opportunity to study collisions between atoms and molecules at very low translational energies. Schemes to produce diatomic molecules in highly excited rotational states have also been proposed [17, 18] and recently realized [19]. Theoretical studies have suggested that the collision dynamics of such rotationally hot molecules would be particularly interesting at low temperatures [20–26]. At low energies, quantum-mechanical effects play a dominant role as the collision dynamics is very sensitive to the intermolecular interaction potential and the relative separation of the initial and final internal energy levels of the scattering partners. Collisions between atoms and rotationally excited diatoms can also cause energy to be transferred between the diatom's internal rotational degrees of freedom. Although translational temperatures typically reach the mK or μK regime or lower, the internal energy may be orders of magnitude larger by comparison. Therefore, the exchange of internal energy during a collision is an important issue in cold and ultracold physics.

Rovibrational energy transfer in atom–molecule collisions has been a topic of a large number of investigations over the past several years. In Balakrishnan *et al* [20], vibrational relaxation cross sections for an atom–molecule system were calculated by explicit numerical solution of the coupled equations of scattering theory and shown to follow an inverse velocity dependence at very low initial kinetic energies of the incident atom in accordance with the Wigner threshold law [27]. Yang *et al* [28–30] found that elastic and inelastic cross sections exhibit sharp resonances at low collision energies for CO scattering with H, He and H_2. As discussed by Bethlem *et al* [14], unusual resonant states can be formed when the colliding molecules begin to rotate, leaving them with insufficient translational energy to overcome their van der Waals attraction. At low velocities, translational energy is transferred due to the anisotropy of the potential energy surface into rotational energy, effectively trapping the molecules transiently by the centrifugal potential. This type of resonance is ubiquitous in cold molecule–molecule collisions because the enormous number of internal molecular states leads to a large number of quasi-bound resonant states. Precise measurements of these resonances yield unprecedented opportunities to study fine details of the potential energy surface of the interacting species. For example, Florian *et al* [25] investigated cold and ultracold collisions involving rotationally excited CO molecules using close-coupling (CC), coupled states (CS) and effective potential approximations. Quenching rate coefficients were given for initial rotational levels near the dissociation threshold. This effort was motivated by the possibility of studying molecular collisions at cold and ultracold temperatures as discussed above.

Since cold and ultracold collisions are very sensitive to intermolecular interaction potentials, accurate potential surfaces for the scattering complexes are very important for reliable theoretical simulations of energy transfer. In this paper, we focus on rotational

transitions in CO by collisions with H, He and H_2 at cold and ultracold temperatures and discuss mechanistic aspects of energy transfer in these systems. Though CO is the common collision partner in all three systems, the interaction potentials and collision dynamics exhibit distinct features. For H–CO, the interaction potential supports the formation of a deeply bound HCO complex which leads to a number of resonances in the energy dependence of elastic and inelastic cross sections. While the interaction potentials for He–CO and H_2–CO are comparable, the additional rotational degrees of freedom in the H_2–CO case as well as the possibility of using *ortho*-H_2 and *para*-H_2 introduce interesting energy transfer pathways. For all these systems, impressive progress has been made in the construction of potential energy surfaces (PESs). For HCO, the BBH [31] and WKS [32, 33] potentials have been extensively used to compute bound state energies as well as scattering dynamics. In the present study, we adopt the more recent WKS PES [32, 33] for H–CO collisions as it provides an improved description of the H–CO interaction. Resonance energies and widths obtained with the WKS potential for HCO and DCO agree well with experiment providing an improvement over previous calculations with the BBH potential [31]. For He–CO collisions, the PES of Heijmen *et al* [34] was adopted. It is considered to be superior to other potentials that are available for this system especially in reproducing the bound state energies of the He–CO complex. A recent comparison by Yang *et al* [29] of cross sections and state-to-state rate coefficients with experiment shows excellent agreement, validating the accuracy of He–CO potential by Heijmen *et al* [34]. For H_2–CO, two versions of the interaction potential have been computed by Jankowski and Szalewicz [35, 36]. The newer potential [36], computed with the coupled-cluster method including single, double and noniterative triple excitations and the supermolecular approach, was adopted here. Comparative studies of collisional cross sections using the two surfaces have been presented in our earlier work [30] and by Wernli *et al* [37]. The updated H_2–CO interaction potential was obtained on a five-dimensional grid including the dependence on the H–H separation while the CO distance was fixed at its vibrationally averaged value resulting from the ground vibrational state of the molecule. The PES was then averaged over the ground state vibrational wavefunction of H_2 to obtain a four-dimensional rigid-rotor potential. Computations of the H_2–CO spectra and second virial coefficients by Jankowski and Szalewicz [36] using the newer potential were found to be in very good agreement with experimental data and an improvement over the previous surface [35].

Unfortunately, available experimental data for these collision systems all probe the relatively short-range part of the interaction potentials which can only give confidence in elastic and inelastic cross sections for collision energies above $\sim$10 cm^{-1}. Recent calculations [21–25] have shown that collisional processes at cold and ultracold temperatures are sensitive to the behaviour of the interaction potentials at intermediate and large internuclear distances. While long-range dispersion coefficients can be calculated accurately with perturbative methods, matching to the intermediate range, usually in the vicinity of a van der Waals well, may be problematic for triatomic and polyatomic systems. Typically, collisional cross sections are strongly influenced by van der Waals interactions at sub-Kelvin temperatures and traditional experimental methods for inelastic processes do not extend down to this temperature regime. Here, we present quantitative investigations of energy transfer in CO by collisions with H, He and H_2 at incident kinetic energies below 10 cm^{-1} where the van der Waals interaction plays an important role. Unlike previous theoretical efforts where collisional properties of a specific system were investigated, we focus here on comparing the behaviour of three different systems with vastly different potential energy surface properties in an effort to elucidate trends that can be explored in future ultracold molecule collision studies.

2. Results and discussion

The theory for atom–diatom and diatom–diatom scattering can be found elsewhere [38–41] while explicit details of the computations of the considered collision systems are listed in our previous papers [28–30]. The calculations presented here were performed by applying both the CC method [38, 40] and the CS approximation [39, 41]. All CC and CS calculations were carried out using the nonreactive scattering code MOLSCAT [42] with the coupled-channel equations integrated using the modified log-derivative Airy propagator of Alexander and Manolopoulos [43] with a variable step size. Calculations were performed for collision energies between 10^{-5} cm^{-1} and 10 cm^{-1}. For initial rotational states j = 20, 30 and 40 of CO, the CS approximation was adopted, while the CC approach was used for all other initial rotational states, $j = 1, 2, \ldots, 10$. The vibrational state for all diatoms is taken to be the ground $v = 0$ level. A sufficient number of total angular momentum partial waves were included at each energy to secure convergence of the cross sections.

While details concerning the basis sets are given in our previous publications [28–30], we mention here that the H_2 basis set included the lowest two rotational states, i.e., $j = 0$ and 2 for *para*-H_2 and $j = 1$ and 3 for *ortho*-H_2. In this work, we only consider excitation of CO and neglect any inelastic processes for H_2. This is a valid approximation for initial rotational states of CO ($j = 1 - 10$) as all H_2 rotational excitation channels are closed for the considered kinetic energies (<10 cm^{-1}). Further, closed-channel couplings are included through the excited H_2 rotational state in the basis. For CO (j = 20, 30 and 40), rotational excitation of H_2 does become possible, and is included in the calculation, but we find that the state-to-state cross sections are typically two orders of magnitude smaller than the corresponding processes where H_2 is elastically scattered. This is in agreement with studies of H_2–H_2 by Forrey [44] where such double diatom transitions were found to give cross sections more than an order of magnitude smaller.

In figure 1, we compare the total quenching cross sections from initial rotational states j = 1, 10 and 40 of CO as a function of the incident kinetic energy due to collisions with H, He, *para*-H_2 and *ortho*-H_2. Generally, all the cross sections from different initial rotational states exhibit the threshold behaviour predicted by Wigner's Law [27] at ultra-low collision energies, where only s-wave scattering contributes and the cross sections vary inversely with the relative velocity. Moreover, figure 1(a) indicates that the Wigner threshold regime occurs at different energies for different colliders reflecting a marked dependence on the interaction potentials. Furthermore, for $j = 1$, the calculations reveal rich resonance structures for scattering with *para*-H_2 and *ortho*-H_2 over the energy range 10^{-1} to 10 cm^{-1} due to the decay of quasi-bound states supported by the van der Waals interaction potential. However, the resonance energies and widths are very different for the two forms of molecular hydrogen. The He–CO cross section also displays a series of resonances, but only for energies above 1 cm^{-1}. On the other hand, the H–CO cross sections are fairly smooth except for some small undulations above 1 cm^{-1}. As discussed by Reid *et al* [45], the low collision energy regime fosters the formation of quasi-bound levels or van der Waals complexes. These long-lived complexes allow multiple collisions to occur thereby strongly enhancing the vibrational and rotational relaxation process and also give rise to open-channel (shape) [46] and closed-channel (Feshbach) [47] resonances. Interestingly, the total quenching cross section for CO scattering with *ortho*-H_2 in the ultra-low energy limit is about a factor of 5 larger than that of CO scattering with *para*-H_2. Further, as noted in our previous study [30], for *para*-H_2 there is a large, but broad resonance near 4×10^{-2} cm^{-1}, but it appears to be significantly suppressed for the *ortho*-H_2 case. The very large cross sections for $j = 1$ for He–CO in the ultracold limit was previously attributed to a Feshbach resonance by Balakrishnan *et al* [22].

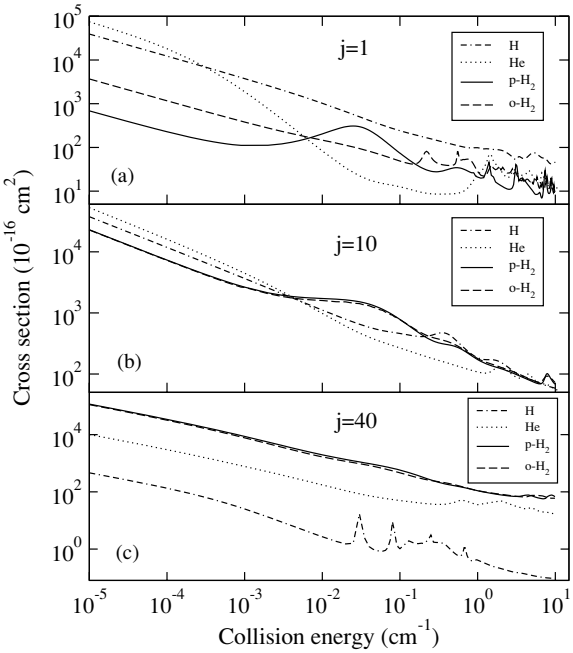

Figure 1. Total quenching cross sections of CO as functions of the incident kinetic energy due to collisions with H, He and H_2 from initial: (a) $j = 1$; (b) $j = 10$ and (c) $j = 40$. Dash-dotted line: CO with H; dotted line: CO with He; solid line: CO with *para*-H_2; dashed line: CO with *ortho*-H_2.

In the quenching of $j = 10$ and 40, figures 1(b) and (c) show, respectively, that the total quenching cross sections for *para*-H_2 and *ortho*-H_2 are very similar over the whole energy range. Both cross sections have a broad resonance below 0.1 cm^{-1}, but the resonance is gradually suppressed with increasing initial j. A similar decrease of shape resonance strength with increasing initial j was found by Zhu *et al* [48] for vibrational quenching of $v = 1$ in ^{3}He–CO collisions and by Yang *et al* [28] for H–CO collisions. For He–CO, figures 1(b) and (c) also show that the resonances become suppressed for $j = 10$ and 40. Conversely for H–CO, the resonance region shifts to smaller collision energies and the resonance amplitudes increase as j increases. This is particularly evident for $j = 40$ for which a number of sharp resonances are present between 10^{-2} and 10^{-1} cm^{-1}. Further, figure 1 shows that the total quenching cross sections are larger for H–CO than those for H_2–CO over the whole energy range for $j = 1$ and at energies below approximately 0.003 cm^{-1} for $j = 10$. Interestingly, for $j = 40$, the quenching cross section for H–CO is smaller than those for H_2–CO and He–CO. These trends can be attributed to the well depths of the collision complexes which are 23.7, 93.0 and 6726 cm^{-1}, respectively, for He–, H_2– and H–CO. Because of their smaller well depths, He–CO and H_2–CO support fewer bound states so that quasi-bound levels correspond to low values of rotational angular momentum quantum numbers. On the other hand, H–CO has a very deep well with a large number of rovibrational bound states. As figure 1(c) illustrates, shape resonances at very-low energies only appear for large j for H–CO. Finally, the close similarity of *para*-H_2 and *ortho*-H_2 for $j = 10$ and 40, unlike the situation for $j = 1$, is due to the lack of quasi-bound levels at these larger values of j.

In figure 2, total quenching cross sections as functions of initial j at collision energies of 10^{-5} and 10^{-1} cm^{-1} are given. Generally, the total quenching cross sections for *para*- and

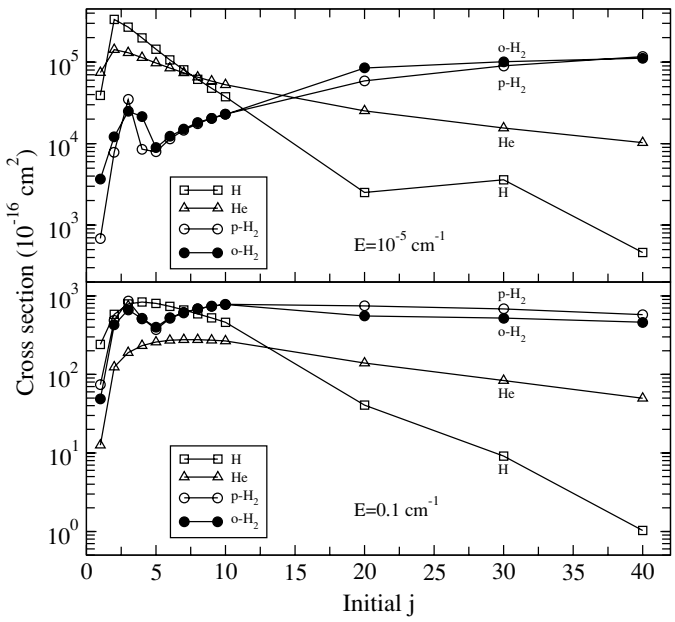

Figure 2. Total quenching cross sections of CO as functions of initial j due to collisions with H, He and H_2 at incident kinetic energies 10^{-5} (upper panel) and 0.1 cm^{-1} (bottom panel). Squares: CO with H; triangle: CO with He; open circles: CO with *para*-H_2; solid circles: CO with *ortho*-H_2. These cross sections are easily converted to total quenching rate coefficients (in cm^3 s^{-1}) by multiplying by 49.57, 26.13, and 35.66 cm s^{-1} for H, He and H_2, respectively, for a collisional energy of 10^{-5} cm^{-1}, for example.

ortho-H_2 have similar behaviours, except for 10^{-5} cm^{-1} for which *ortho*-H_2 results for $j = 1$ and 4 are larger than those for *para*-H_2. At both energies, the total quenching cross sections increase initially from $j = 1$ and exhibit peaks at $j = 3$. After $j = 5$, the cross sections vary slowly with increasing initial j.

For H–CO and He–CO, the total quenching cross sections as a function of j are similar, but different from those for H_2–CO. At a collision energy of 10^{-5} cm^{-1}, the cross section for $j = 1$ is smaller than that for $j = 2$. Then the cross sections generally decrease with increasing j. For 10^{-1} cm^{-1}, the cross sections increase initially and reach maximum values at $j = 3$ for H–CO and at $j = 7$ for He–CO, and decrease monotonously to $j = 40$. The total quenching cross sections for H–CO are larger than those for H_2–CO at lower initial j and smaller at larger initial j. While figure 2 does point out some similarities in the quenching cross sections for the considered collision systems, significant differences are apparent. These differences stem from the vast differences in the potential energy surfaces and not from the mass differences of the collision partners.

Examples of state-to-state quenching cross sections for collision energies of 10^{-5} and 10^{-1} cm^{-1} are shown in figures 3–6 for CO scattering with H, He, *para*-H_2 and *ortho*-H_2, respectively. For all initial rotational levels, the quenching cross sections show a general decrease with increasing $\Delta j = |j' - j|$. Superimposed on this general trend, there are also some oscillations with Δj for low rotational states, with a propensity for odd Δj or even Δj.

In all cases and over most of the considered energy range, the quenching cross sections are dominated by $\Delta j = -1$ transitions, a trend similar to that noted for the He–CO system [26] where the cross sections increase with decreasing CO rotational energy gap between initial and

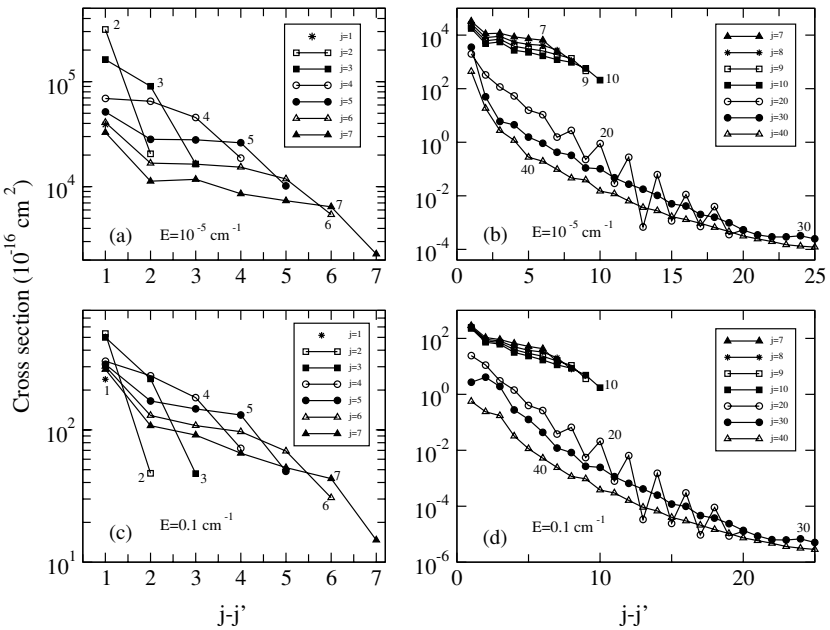

Figure 3. Quenching cross sections of CO due to collisions with H as functions of $j - j'$ from initial $j = 1$–10, 20, 30 and 40 at collision energies 10^{-5} (a and b) and 0.1 cm^{-1} (c and d). In (a) and (c), stars are for $j = 1$, open squares $j = 2$, solid squares $j = 3$, open circles $j = 4$, solid circles $j = 5$, open triangles $j = 6$ and solid triangles $j = 7$. In (b) and (d), solid triangles are for $j = 7$, stars $j = 8$, open squares $j = 9$, solid squares $j = 10$, open circles $j = 20$, solid circle $j = 30$ and open triangles $j = 40$.

final states. The oscillatory behaviour of the cross sections is due to the competition between even and odd order terms in the Legendre polynomial expansion of the interaction potential. The preference for odd over even Δj has been discussed by Carty *et al* [49] and McCurdy *et al* [50] and it occurs due to the strong anisotropy of the He–CO interaction potential. This propensity, however, is not evident at larger Δj for He–CO and H_2–CO. For the case of CO with H, figure 3 shows that the quenching cross section from $j = 20$ displays strong oscillations at high Δj. The oscillations for $j = 30$ and 40 are not as evident as those for $j = 20$.

Comparing the state-to-state cross sections for the four collision systems, there is a general trend for an increase in the cross sections with initial j for a given Δj for *para*-H_2 and *ortho*-H_2 (primarily for $\Delta j > 3$). A similar trend is suggested for He collisions, except for an apparent turn-over for the largest few Δj. Conversely, for H–CO the opposite trend is evident with the cross sections decreasing with increasing j. This is likely to be related to the significantly larger binding energy of the H–CO complex.

For low energies, a simple interpolation method may be used to compute energy-dependent cross sections for a desired initial state from ones already computed for a different initial state. Take CO scattering with He as an example, the interpolation formula

$$\sigma(j, j - \Delta j; E) = \sigma(j, j - \Delta j; E = 0)\frac{\sigma(20, 20 - \Delta j; E)}{\sigma(20, 20 - \Delta j; E = 0)} \tag{1}$$

was used to estimate $\sigma(30, 30 - \Delta j; E)$ from a single $E \approx 0$ calculation for $j = 30$ and $\sigma(20, 20 - \Delta j; E)$ which provides the energy dependence. The results are shown in figure 7. Solid curves are the interpolated values and the points are the actual computed values. Wigner

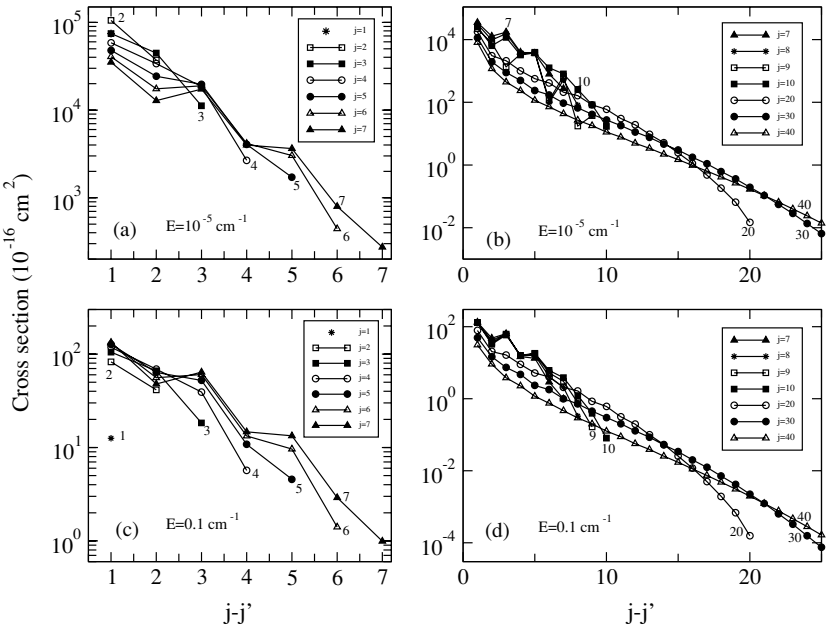

Figure 4. Same as in figure 3, except for He–CO.

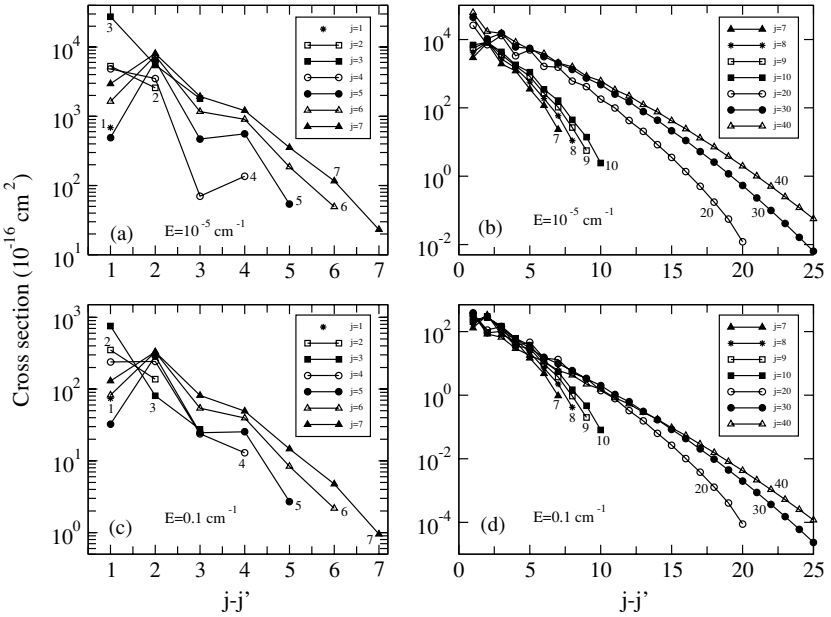

Figure 5. Same as in figure 3, except for *para*-H_2–CO.

threshold behaviour is exactly reproduced by this kind of interpolation. The cross sections have been multiplied by collision velocity in order to better illustrate the onset of variations from the threshold law. Because the energy and angular momentum gaps between initial and

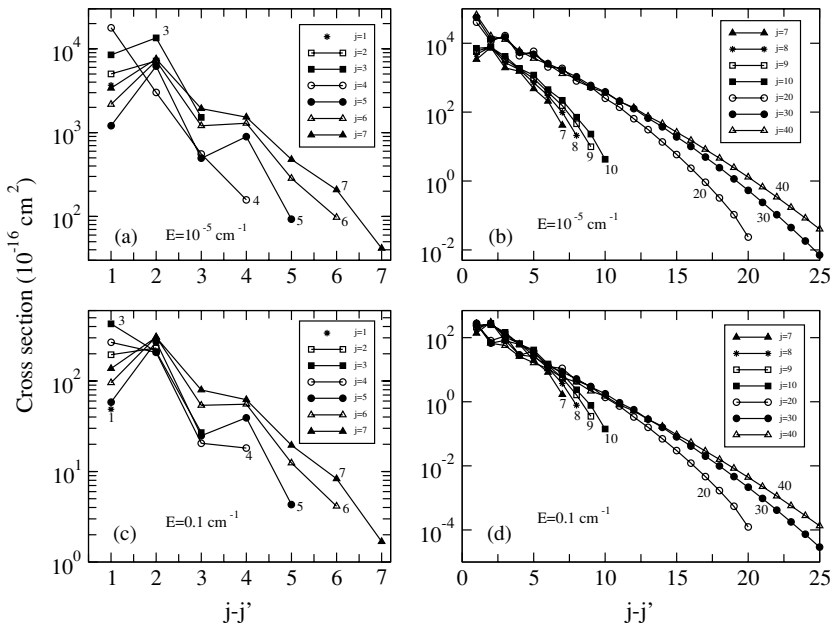

Figure 6. Same as in figure 3, except for *ortho*-H_2–CO.

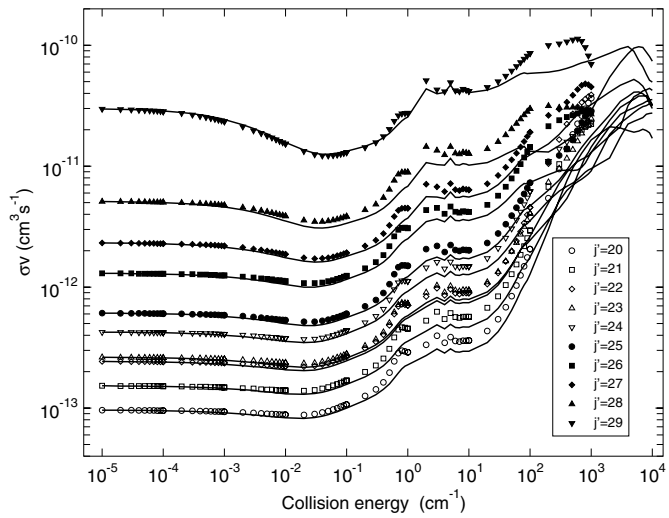

Figure 7. Energy-dependent state-to-state rate coefficients of CO ($j = 30$) due to collisions with He. The points are computed values of coupled-states calculations. The curves are interpolated values obtained from equation (1).

final states are approximately the same, the interpolation method provides reasonable estimates of the actual cross sections for energies up to 100 cm^{-1}. The method generally improves as the j-value of the reference cross section approaches that of the interpolated cross section and

offers a practical means to compute a large amount of data from a small number of program executions without using intractably large basis sets.

In the present study, we have explored the effect of pure rotational transitions in all four considered collision systems. While we have primarily illustrated the trends graphically, in future work, with a complete set of initial j cross sections, we will investigate the physical mechanisms of the cross section behaviours. Such analyses will draw upon dynamically based angular momentum and energy gap scaling laws [51]. When vibrational degrees of freedom are also included vibrational transitions may reveal interesting quasiresonant behaviour as observed in previous studies of the He–H_2 system [24]. Such effects will be especially interesting for molecule–molecule collisions as in the case of the H_2–CO system. Currently, we are in the process of incorporating vibrational degrees of freedom in our close-coupling approach. While the H_2–CO potential adopted in the present study does not include vibrational degrees of freedom, we expect that such potential energy surfaces will become available in the near future. Full-dimensional potential energy surfaces have been developed for the H_2–H_2 system and we are in the process of implementing our procedure for H_4 and its isotopic counterparts.

3. Conclusion

Collisional energy transfer in cold and ultracold molecules is very sensitive to the intermolecular potential. As examples we have investigated cold and ultracold collisions involving rotationally excited CO with H, He and H_2 using an explicit quantum-mechanical close-coupling approach and the coupled-states approximation. State-to-state quenching cross sections of CO from $j = 1, 2, \ldots, 10, 20, 30$ and 40 show resonance structures at low energies due to the formation of van der Waals complexes for He–CO and H_2–CO, and due to the formation of a strongly bound HCO complex for the H+CO system. We believe that the illustrative results presented here will benefit future experimental studies of these or similar systems as methods to cool and trap neutral polar molecules become more robust and widespread.

Acknowledgments

BY and PCS acknowledge support from NASA grant NNG04GM59G. NB acknowledges support from NSF through grant PHY-0555565 and the Research Corporation. RCF acknowledges support from the NSF through grant PHY-0554794 and a grant to ITAMP at Harvard University and Smithsonian Astrophysical Observatory. Some of the calculations were performed on the IBM p655 High Performance Computer of the UGA Research Computing Center.

References

[1] Doyle J, Friedrich B, Krems R V and Masnou-Seeuws F 2004 *Eur. Phys. J.* D **31** 149
[2] Krems R V 2005 *Int. Rev. Phys. Chem.* **24** 99
[3] Doyle J M, Friedrich B, Kim J and Patterson D 1995 *Phys. Rev.* A **52** R2515
[4] Weinstein J D, deCarvalho R, Guillet T, Friedrich B and Doyle J M 1998 *Nature* **395** 148
[5] Egorov D, Lahaye T, Schollkopf W, Friedrich B and Doyle J M 2002 *Phys. Rev.* A **66** 043401
[6] Fioretti A, Comparat D, Crubellier A, Dulieu O, Masnou-Seeuws F and Pillet P 1998 *Phys. Rev. Lett.* **80** 4402
Nikolov A N, Eyler E E, Wang X, Wang H, Li J, Stwalley W C and Gould P L 1999 *Phys. Rev. Lett.* **82** 703
Takekoshi T, Patterson B M and Knize R J 1999 *Phys. Rev.* A **59** R5
[7] Wynar R, Freeland R S, Han D J, Ryu C and Heinzen D 2000 *Science* **287** 1016

[8] Fioretti A, Fazzi M, Mazzoni M, Ban T and Gabbanini C 2004 *Phys. Scr.* T **112** 13
Stwalley W C and Uang Y H 1999 *J. Mol. Spectrosc.* **195** 194
[9] Greiner M, Regal C A and Jin D S 2003 *Nature* **426** 537
[10] Zwierlein M W, Stan C A, Schunck C H, Raupach S M, Gupta S, Hadzibabic Z and Ketterle W 2003 *Phys. Rev. Lett.* **91** 250401
[11] Regal C A, Greiner M and Jin D S 2004 *Phys. Rev. Lett.* **92** 040403
[12] Bartenstein M, Altmeyer A, Riedl S, Jochim S, Chin C, Denschlag J H and Grimm R 2004 *Phys. Rev. Lett.* **92** 120401
[13] Bethlem H L, Berden G and Meijer G 1999 *Phys. Rev. Lett.* **83** 1558
[14] Bethlem H L, Berden G, Crompvoets F M H, Jongma R T, van Roij A J A and Meijer G 2000 *Nature* **406** 491
Bethlem H L and Meijer G 2003 *Int. Rev. Phys. Chem.* **22** 73
[15] Crompvoets F M H, Bethlem H L, Kupper J, van Roij A J A and Meijer G 2004 *Phys. Rev.* A **69** 063406
[16] van de Meerakker S Y T, Smeets P H M, Vanhaecke N, Jongma R T and Meijer G 2005 *Phys. Rev. Lett.* **94** 023004
[17] Karczmarek J, Wright J, Corkum P and Ivanov M 1999 *Phys. Rev. Lett.* **82** 3420
[18] Li J, Bahns J T and Stwalley W C 2000 *J. Chem. Phys.* **112** 6255
[19] Villeneuve D M, Aseyev S A, Dietrich P, Spanner M, Ivanov M Y and Corkum P B 2000 *Phys. Rev. Lett.* **85** 542
[20] Balakrishnan N, Forrey R C and Dalgarno A 1997 *Chem. Phys. Lett.* **280** 1
[21] Balakrishnan N, Forrey R C and Dalgarno A 1998 *Phys. Rev. Lett.* **80** 3224
[22] Balakrishnan N, Dalgarno A and Forrey R C 2000 *J. Chem. Phys.* **113** 621
[23] Forrey R C, Balakrishnan N, Kharchenko V and Dalgarno A 1998 *Phys. Rev.* A **58** R2645
[24] Forrey R C, Balakrishnan N, Dalgarno A, Haggerty M and Heller E J 1999 *Phys. Rev. Lett.* **82** 2657
[25] Florian P M, Hoster M and Forrey R C 2004 *Phys. Rev.* A **70** 032709
[26] Bodo E, Gianturco F A and Dalgarno 2002 *Chem. Phys. Lett.* **353** 127
[27] Wigner E P 1948 *Phys. Rev.* **73** 1002
[28] Yang B, Stancil P C and Balakrishnan N 2005 *J. Chem. Phys.* **123** 094308
[29] Yang B, Stancil P C, Balakrishnan N and Forrey R C 2005 *J. Chem. Phys.* **123** 134326
[30] Yang B, Stancil P C, Balakrishnan N and Forrey R C 2006 *J. Chem. Phys.* **124** 104304
[31] Bowman J M, Bittman J S and Harding L B 1986 *J. Chem. Phys.* **85** 911
[32] Werner H-J, Bauer C, Rosmus P, Keller H-M, Stumpf M and Schinke R 1995 *J. Chem. Phys.* **102** 3593
[33] Keller H-M, Floethmann H, Dobbyn A J, Schinke R, Werner H-M, Bauer C and Rosmus P 1996 *J. Chem. Phys.* **105** 4983
[34] Heijmen T G A, Moszynski R, Wormer P E S and van der Avoird A 1997 *J. Chem. Phys.* **107** 9921
[35] Jankowski P and Szalewicz K 1998 *J. Chem. Phys.* **108** 3554
[36] Jankowski P and Szalewicz K 2005 *J. Chem. Phys.* **123** 104301
[37] Wernli M, Valiron P, Faure A, Wiesenfeld L, Jankowski P and Szalewicz K 2006 *Astron. Astrophys.* **446** 367
[38] Arthurs A and Dalgarno A 1960 *Proc. R. Soc. Lond.* A **256** 540
[39] McGuire P and Kouri D J 1974 *J. Chem. Phys.* **60** 2488
[40] Green S 1975 *J. Chem. Phys.* **62** 2271
[41] Heil T G, Green S and Kouri D J 1978 *J. Chem. Phys.* **68** 2562
[42] Hutson J M and Green S 1994 *MOLSCAT Computer Code* version 14, distributed by Collaborative Computational Project 6 of the Engineering and Physical Sciences Research Council, UK
[43] Alexander M H and Manolopoulos D E 1987 *J. Chem. Phys.* **86** 2044
[44] Forrey R C 2001 *Phys. Rev.* A **63** R051403
[45] Reid J P, Simpson C J S M and Quiney H M 1997 *J. Chem. Phys.* **107** 9929
[46] Toennies J P, Welz W and Wolf G 1979 *J. Chem. Phys.* **71** 614
[47] Micha D A 1967 *Phys. Rev.* **162** 88
[48] Zhu C, Balakrishnan N and Dalgarno A 2001 *J. Chem. Phys.* **115** 1335
[49] Carty D, Goddard A, Sims I R and Smith I W M 2004 *J. Chem. Phys.* **121** 4671
[50] McCurdy C W and Miller W H 1977 *J. Chem. Phys.* **67** 463
[51] Steinfeld J I, Ruttenberg P, Millot G, Fanjoux G and Lavorel B 1991 *J. Phys. Chem.* **91** 9638